START-TO-END SIMULATION OF A SMITH-PURCELL FREE ELECTRON LASER*

C. Prokop[1], P. Piot[1,2], M. C. Lin[3], P. Stoltz[3]
[1] Department of Physics, Northern Illinois University DeKalb, IL 60115, USA
[2] Fermi National Accelerator Laboratory, Batavia, IL 60510, USA
[3] Tech-X Corporation, Boulder, CO 80303, USA

Abstract

Terahertz (THz) radiation has generated much recent interest due to its ability to penetrate deep into many organic materials without the damage associated with ionizing radiations. Smith-Purcell free-electron lasers (SPFELs) offer a viable path toward generating copious amounts of narrow-band THz radiation. In this paper we present numerical simulations, performed with the conformal finite-difference time-domain electromagnetic solver VORPAL of a SPFEL operating in the superradiant regime. We first explore the standard (single grating) configuration and investigate the impact of incoming beam parameters. We also present a new concept based a double grating configuration to efficiently bunch the electron beam, followed by a single grating to produce super-radiant SP radiation.

INTRODUCTION

Terahertz (THz) radiation is finding use in an increasingly wide variety of applications including medical imaging, homeland security and global environment monitoring [1]. Increasing access to THz technologies requires the development of compact and tunable THz sources. Recent years have witnessed a resurgence of interest in Smith-Purcell free-electron lasers (SPFELs) operating as a backward wave oscillator [2, 3] following on an idea initially discussed in Ref. [4]. The developed model was recently benchmarked by laboratory experiments [5, 6]. THz sources based on SPFELs are foreseen to have table-top footprint and can operate in a continuous wave mode, enabling the production of moderate average output power (on the order of Watts).

In an SPFEL, a low energy ($\sim$ 50 keV) sheet DC electron beam is propagated close to a metallic grating with velocity $\mathbf{v} \equiv c\beta\hat{y}$. The beam excites evanescent surface waves with axial field of the form $E_{y,e}(x,y) = E_{0,e}\exp(\alpha x)$ where $\alpha \equiv 2\pi/(\beta\gamma\lambda_e)$ and $\gamma \equiv (1-\beta^2)^{-1/2}$ is the Lorentz factor. The evanescent wave can, under certain circumstances, have a negative group velocity [2]. In such a case the wave counter-streams the electron beam direction and can couple to the beam, thereby giving rise to an energy modulation. Due to the non-relativistic nature of the beam ($\gamma \simeq 1$), the energy modulation eventually transforms into a density modulation at wavelength λ_e. The produced microbunches will result in strongly enhanced radiation at harmonic frequencies of the microbunching frequency $f_e \equiv c/\lambda_e$. In an SPFEL the radiative mechanism is the Smith-Purcell (SP) effect [7]. If instead of a DC electron beam, a beam consisting of a train of microbunches is used the SP radiation is emitted in the superradiant regime [8, 9, 10] in which the radiation rate goes as the number of electrons in each microbunch squared. Prebunching the electron beam in a way that satisfies emission of super-radiant radiation is however challenging and several solutions have been discussed in, Ref. [11, 12, 16].

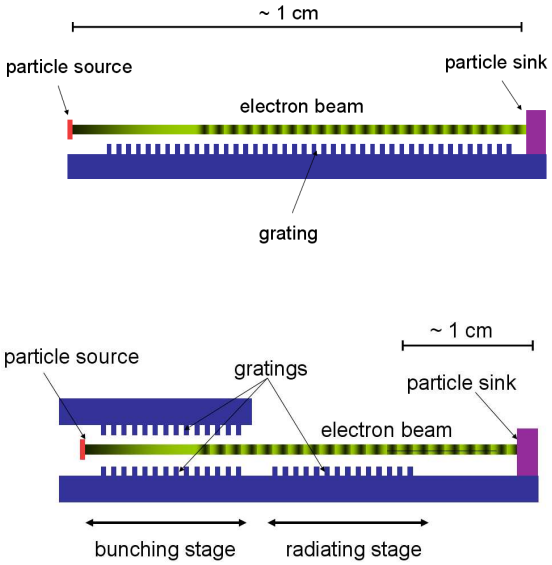

Figure 1: Diagrams of the two systems considered in this paper: the single-grating configuration (top) and the two-stage configuration (bottom). Blue blocks represent conducting material. The entire computational domain is surrounded by perfectly-match layers (PMLs) to emulate open boundary conditions.

In this paper, we first explore via simulations the effect of velocity spread on the performances of a conventional SPFEL. We then elaborate on a possible improvement using a dual-grating configuration. The simulations were per-

*This work was partially supported by the US Department of Education under contract number P116Z050086 with Northern Illinois University.

Table 1: Grating and beam parameters used for the VORPAL simulations.

Parameter	Symbol	Value	Unit
Grating Period	λ_g	200	μm
Groove Width	w	100	μm
Groove Depth	h	100	μm
Number of Periods/grating	N_g	75	$--$
Electron Energy	E	50	keV
Beam Current	I	1000	A/m
Beam Thickness	b	20	μm
Beam Clearance	g	20	μm
Fractional Energy Spread	g	$0-1$	%
Transverse Emittance	ε_x	$0-10$	μm
External Magnetic Field	B_a	2.0	T
Electrons per Macro Particle	$-$	10^6	$-$

formed with the conformal finite-difference time-domain electromagnetic solver, VORPAL [13].

BEAM PARAMETERS IMPACT ON A SINGLE-GRATING SPFEL

We consider the single-grating SPFEL shown in Fig. 1 (top). Most of the numerical simulations performed to date assumes a "cold" beam model. The simulations are two dimensional and used the same model detailed in Ref. [16]: the DC beam is taken to have a uniform horizontal (along x) density with width b. To characterize the beam, we introduce the transverse normalized emittance $\varepsilon_x \equiv 1/(mc)[\langle x^2\rangle\langle p_x^2\rangle - \langle xp_x\rangle^2]^{1/2}$. Assuming no position-momentum correlation in the emitted beam (so that $\langle xp_x\rangle = 0$) we associate the uncorrelated transverse velocity spread $\langle v_x^2\rangle^{1/2} = c\varepsilon_x\sqrt{12}/b$. We quantify the effect of longitudinal velocity spread by introducing a velocity spread taken as a percentage of the average beam velocity. For these simulations, the beam is born and transported in a magnetic field with a uniform axial component.

The SPFEL mechanism operates in a manner similar to a high-gain amplifier: as the beam propagates above the grating the electromagnetic fields associated (both associated to the evanescent and radiative fields) grows as $\{E,B\}(t) = \{E_0,B_0\}\exp(t/\tau)$, where τ^{-1} is the growth rate. The FEL process eventually saturates and the field amplitudes become constant, i.e. $\{E,B\}(t\rightarrow\infty) = \{E_\infty,B_\infty\}$. In the following we define the gain as $\mathcal{G} \equiv E_\infty/E_0$.

The growth rate is computed from the magnetic field history recorded at a point 4.5 mm from the center of the grating, at an angle of 105 degrees with the beam direction corresponding to the angle at which maximum SP radiation is expected from the SP equation [7] and the dispersion relation [2].

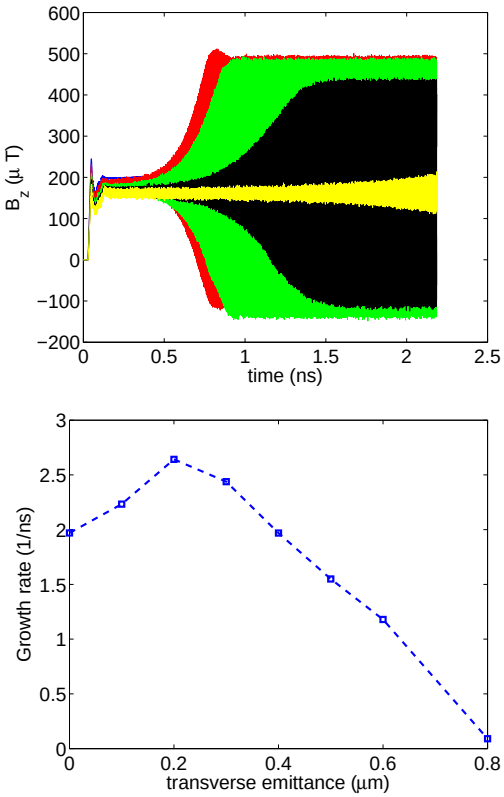

Figure 2: Histories of the magnetic field (top) recorded for (blue) 0, (red) 0.2, (green) 0.4, (black) 0.6, and (yellow) 0.8 μm normalized transverse emittance and corresponding growth rate (bottom).

To extract the growth rate from the field history, a MATLAB program was developed that scanned over the history data with a user-defined frame size, and calculated the exponential growth rate for each frame via a fit. The growth rate evolution as a function of transverse emittance and fractional energy spread are respectively reported in Figs. 2 and 3. As expected, an increase in either tranverse emittance or fractional energy spread reduces the growth rate. The gain is however weakly affected by the increases in emittance or fractional energy spread (a growth rate decrease by a factor 2 has an associated gain reduction of 20 % only). From these simulations, which include a external focusing provided by a 2 T uniform axial (along the $\hat{y}$-axis) magnetic field, we infer the required transverse emittance and fractional energy spread to be respectively $\varepsilon_x \leq 0.5\,\mu$m and $\sigma_\delta \leq 0.3$ %. These parameters are within reach of field emission or thermionic electron sources.

TWO-STAGE CONFIGURATION

Recently we explored the performance of a two-stage SPFEL depicted in Fig. 1 (bottom). A first stage referred to as "buncher" includes a pair of grating to maximize the bunching efficiency. The microbunched beam is then passed through a single grating referred to as "radiator" and

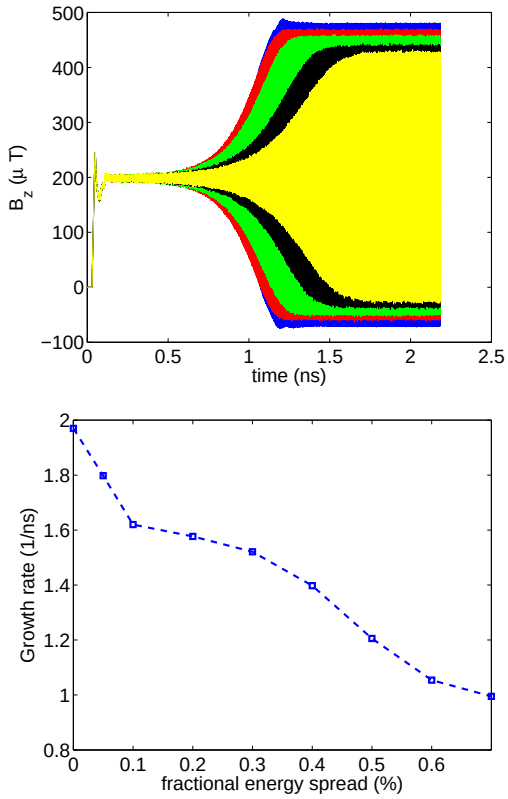

Figure 3: Histories of the magnetic field (top) recorded for (blue) 0, (red) 0.2, (green) 0.4, (black) 0.6 % and (yellow) 0.7 % fractional energy spread and associated growth rate (bottom).

produce super-radiant SP radiation. . The performances of this two-stage SPFEL were investigated in Ref. [16].

The two main features of the two-stage configuration are (1) the strengthened evanescent field that may be taken advantage of to relax the start current requirements and (2) the dual grating configuration results to a different dispersion relation than for the single-grating configuration. This feature offers a greater flexibility for tuning the evanescent wave frequency (and therefore the radiation frequency) by either varying the electron beam energy, or altering the gap between the two gratings in the "buncher" section; see Fig. 4.

FUTURE PLANS

Our research plans eventually include the construction of a table top THz radiation source using a DC gun already built at Northern Illinois University. Based on the studies carried so far, we foreseen to build a two-stage SPFEL pending the final analysis of its sensitivity to beam emittance and energy spread.

In the near future we plan on improving our VORPAL simulation to start with a macroparticle distribution (and associated fields) generated with ASTRA, the tracking code used to design the electron source.

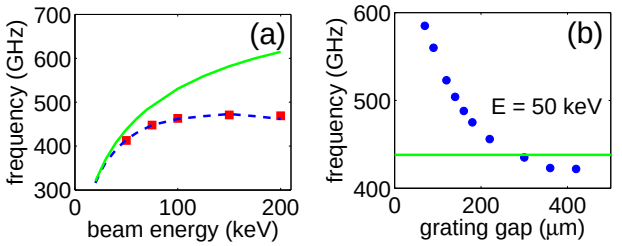

Figure 4: Evanescent wave frequency versus beam energy for the single-grating configuration (a) and evanescent wave frequency versus grating separation for a double-grating configuration (b). The markers are results from VORPAL simulations while the dashed line is obtained from the dispersion relation derived in Ref. [2]. In both graphs, the green solid line denotes the minimum allowed SP frequency for a grating period of 200 μm (from reference [16]).

REFERENCES

[1] M. Tonouchi, *Nature Photonics*, **1**, 97-105 (2007).

[2] H. L. Andrews and C. A. Brau, *Phys. Rev. ST Accel. Beams*, **7**, 070701 (2004).

[3] V. Kumar and K.-J. Kim, *Phys. Rev. E* **73**, 026501 (2006).

[4] J. M. Wachtel, *J. Appl. Phys.*, **50** (49) (1979).

[5] H. L. Andrews and C. A. Brau, Phys. Rev. ST Accel. Beams **12**, 080703 (2009).

[6] J. T. Donohue, L. Courtois, P. Modin, and J. Gardelle, *Phys. Rev. ST Accel. Beams* **12**, 110701 (2009)

[7] S. J. Smith and E. M. Purcell, *Phys. Rev.* **92**, 1069 (1953).

[8] H. L. Andrews, C.H. Boulware, C.A. Brau, J.D.. Jarvis, Proceedings of the 26th International Free Electron Laser Conference, Trieste, Italy, 29 August - 3 September, 2004, pp. 278-281.

[9] D. Li, K. Imasaki, Z. Yang, and G.S. Park, *Appl. Phys. Lett.* **88**, 201501 (2006).

[10] A. Kesar, R. Marsh, R. Temkin, *Phys. Rev. ST Accel. Beams* **9**, 022801 (2006).

[11] Y. Li and K.-J. Kim, *Appl. Phys. Lett.* **92**, 014101 (2008).

[12] Z. Shi, Z. Yang, F. Lan, X. Gao, Z. Liang, and D. Li, *Nuc. Instr. Meth. A* **607**, 367-371 (2009).

[13] C. Nieter and J. R. Cary, *J. Comp. Phys.*, **196**, 448 (2004).

[14] J. T. Donohue and J. Gardelle, *Phys. Rev. ST Accel. Beams* **8**, 060702 (2005).

[15] C. R. Prokop, P. Piot, M. C. Lin, and P. Stoltz, Proceedings of the 31st Free Electron Laser Conference, Liverpool, UK, 23-28 August, 2009, pp. 180-183.

[16] C. R. Prokop, P. Piot, M. C. Lin, and P. Stoltz, *Applied Physics Letters* **96**, 151502 (2010)

[17] H. P. Freund and T. M. Abu-Elfadl, *IEEE Trans. Plasma Sci.*, **32**, 1015 (2004).

[18] J. S. Nodvick and D. S. Saxon, *Phys. Rev.* **96**, 180 (1954).